Amercian Mineralogist, Volume 58, pages 172-188, 1973

Unusual Titanian-Chromian Spinels from the Eastern Bushveld Complex

EUGENE N. CAMERON AND EVERETT D. GLOVER

Department of Geology and Geophysics, University of Wisconsin, Madison, Wisconsin 53706

Abstract

Spinels in mafic replacement pegmatites of the eastern Bushveld Complex form an unbroken series from Ti-poor chromite to Cr-poor titanomagnetite. The series is characterized by progressive substitution of Fe and Ti for Mg, Al, and Cr. The general ranges in oxide contents are: TiO_2, 0.82 to 20.09 percent; Al_2O_3, 0.68 to 20.49 percent; Cr_2O_3, 0.42 to 43.74 percent; V_2O_3, 0.40 to 3.90 percent; Fe_2O_3, 3.5 to 34.56 percent; FeO, 23.71 to 51.30 percent; and MgO, 0.43 to 7.66 percent. However, magnesian chromian hercynites with Al_2O_3 up to 55.91 are present in some specimens, and one specimen contains Fe-Ti-rich spinels with as much as 10 percent V_2O_3. The series is similar to that reported from lavas of Makaopuhi, Hawaii, and is a ferrian counterpart of the chromite-ulvöspinel series now known from lunar rocks.

Nearly the full range of composition is found in massive oxide layers at contacts of mafic pegmatites with various chromitite layers of the Critical Zone. Such layers have formed mainly by reaction of pegmatite fluids with chromitite during replacement of silicate rocks, but a stage of solid diffusion is indicated by the pattern of cation distribution across the oxide layers.

The spinels bridge the compositional gap between the Ti-poor chromites of the lower part of the Bushveld Complex and the titanomagnetites of the upper part. Inferences as to the role of clinopyroxene crystallization in inhibiting spinel formation during accumulation of the middle part of the Bushveld sequence are thereby strengthened.

Introduction

Titanomagnetite and chromite are well known from thousands of occurrences in terrestrial igneous rocks, but spinels intermediate in composition between titanomagnetite and chromite are decidedly uncommon. They have been found in lavas but have been reported in deeper-seated rocks only from the Bushveld Complex.

Spinels transitional between titanomagnetite and chromite were first described from the Bushveld by J. J. Frankel (1942). Frankel gave partial chemical data including two analyses of intermediate spinels from one of the mafic pegmatites that occur in the eastern Bushveld. Some of these pegmatites were later described by Cameron and Desborough (1964). In numerous specimens from the pegmatites, the presence of spinels ranging from titanomagnetite to chromite was inferred from reflectivity and microhardness measurements, from color changes, and from variations in unit cell size. Further microscope studies have now been made, and the spinels have been analyzed by means of the electron microprobe. The results are presented in this paper.

Materials Studied

Materials studied were collected from pegmatite bodies on Farms Annex Grootboom, Tweefontein, and De Grooteboom, described by Cameron and Desborough, and from two additional bodies on Annex Grootboom (Fig. 1). The bodies range from a few to more than 400 m across. All have formed by replacement of the layered rocks of the Critical Zone. The rock sequence involved consists of interlayered pyroxenite, norite, and anorthosite units, with intercalated chromitite layers ranging from a few mm to as much as 2 m in thickness. The reader is referred to the paper by Cameron and Desborough (1964) for a more detailed discussion of the rock sequence and the pegmatite bodies.

Methods of Study

Standard methods of microscope study were used to investigate about 150 polished sections and slabs cut from samples of various pegmatite bodies and pegmatite-chromitite contact zones. Selected samples were then analyzed by means of the electron microprobe, first for Ti, Fe, and Mg, then for Cr, V, and Al, using an ARL-EMX microprobe operating at 15 kV. The Kα X-rays for each set of three ele-

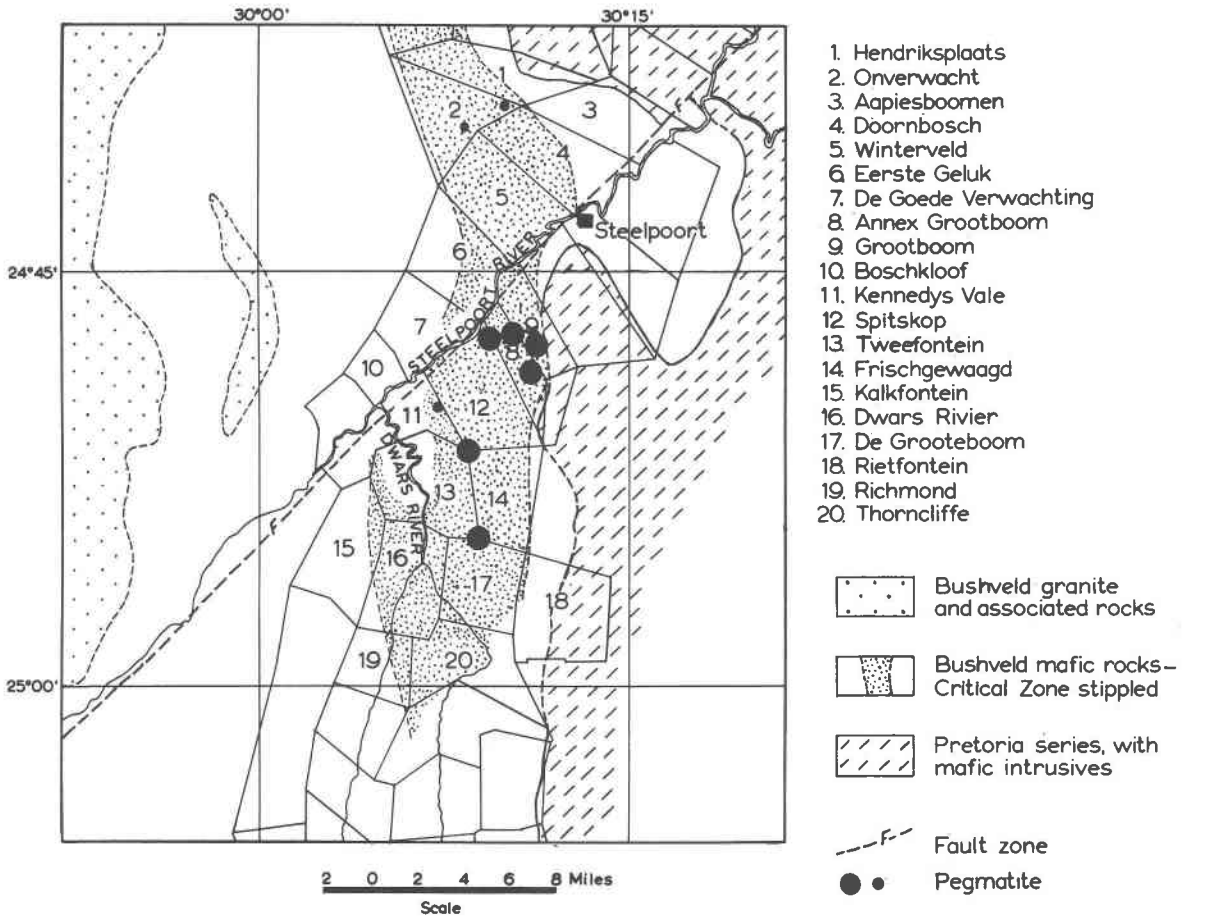

FIG. 1. Generalized geologic map of part of the eastern Bushveld Complex, showing locations of pegmatites from which samples were taken for this paper.

ments were counted and referred to similar counts on standards. Integrated 'beam current' was used for counting control. Standards used were synthetic TiO_2, synthetic MgO, natural hematite containing 1 percent TiO_2, a wet-chemically analyzed Bushveld chromite, vanadium metal, and synthetic corundum.

A photograph of each crystal served to fix locations of points analyzed. Some crystals analyzed are homogeneous, hence presented no problem of precise location of the beam for the two stages of analysis. Other crystals are fine-scale intergrowths of magnetite and ulvöspinel. Counts on these were taken at 5 to 10 randomly selected spots; duplicate analyses and summations indicate that errors in such analyses are within the normal range for microprobe analysis. Still other crystals are intergrowths of magnetite, ilmenite, and ulvöspinel, or of magnetite, hercynite, and ulvöspinel or ilmenite. In many of these, components are smaller than the minimum diameter of the electron beam; hence analysis of aggregates is unavoidable. Two methods of analysis have been tried: (1) defocusing the beam to 10 to 50 μm in diameter, and (2) analyzing a large number of spots, randomly selected or on traverse across crystals, with the normal beam. Results by the two are in close agreement ($\pm$ 2 to 5 percent, relative basis), but summations commonly range from 102 to 104 percent.

Specimens across chromitite-pegmatite contact zones show rapid change in composition. Indentations made with a Leitz Durimet microhardness tester were photographed and used for precise control of the locations of points analyzed.

The Al Kα X-ray levels were measured on some samples using the PHA system in the differential mode to avoid Cr Kα, third order interference. On other samples, the integral mode was used and the Al concentrations were corrected by a predetermined factor.

Where small amounts of vanadium were present, the Kα peak of vanadium was partially masked by the Ti Kβ peak. The vanadium count had therefore to be corrected for this interference by a separate routine. The correction factors necessary to be applied to the vanadium Kα count for several Ti/V ratios were determined by point counting over the V Kα — Ti Kβ wavelength range, then subtracting the Ti Kβ distribution from the V Kα distribution to obtain the net V Kα count at the peak maximum. The ratio of the net V Kα count to that measured was applied to correct the measured V Kα count for each sample.

Correction of the X-ray data for electron and X-ray in-

teractions was done for the five major elements, where the V concentration was low, using the University of Wisconsin computer programs 'Proban' or 'Genie 2,' which reduce data and correct it by the Bence and Albee empirical method. This does not correct for vanadium. The samples with larger V contents were corrected using the programs 'Progsf' or 'Genie 1,' which apply the University of Wisconsin data reduction routine but correct by a modified version of the Goldstein—Comella theoretical correction program. These latter programs were also used to determine correction factors to apply to the lower vanadium count ratios where the other five elements were corrected by the Bence and Albee method. Corrections by the two methods for the five major elements were not significantly different in terms of limits of error stated below.

The assignment to formulae of the unnormalized concentrations obtained was done with a short computer program, 'Spinel.' All titanium was assigned to an ulvöspinel formula, with the other elements first filling the ulvöspinel formula, then being apportioned to the normal spinel formula using Fe partition into Fe^{+2} or Fe^{+3} to give charge balance.

Since the Fe^{+2}/Fe^{+3} apportioning of the Fe was used to calculate the formulae, stiochiometry can not be used as a measure of the accuracy of the analysis. However, the oxide totals, after apportioning the iron, lie generally between 98.0 and 102.0 percent, and this gives some measure of the accuracy. We believe the error range to be ± 2 percent, relative basis, for the higher concentrations and ± 5 percent, relative basis, for the lower concentrations.

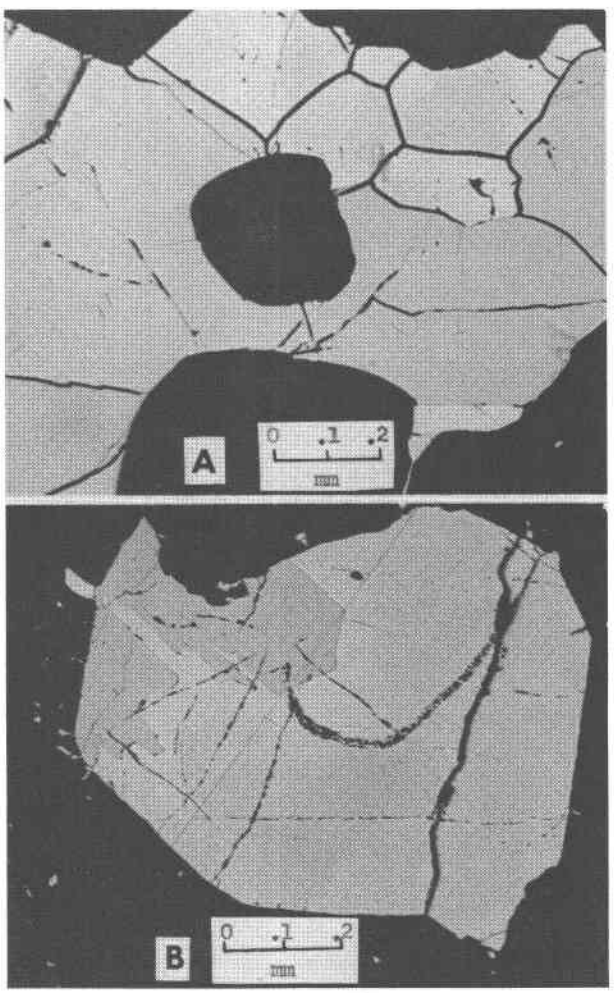

FIG. 2. (a) Granular ilmenite (light gray) interstitial to silicates (black). Oil imm.

(b) Ilmenite (upper left, medium gray) apparently replaced along (0001) by magnetite-ulvöspinel (lighter gray). Oil imm.

Oxide Mineral Assemblages

There are two principal types of oxide mineral assemblages related to the pegmatites studied: 1) assemblages within the pegmatite bodies, and 2) assemblages at contacts of pegmatite with various chromitite layers. These two assemblages differ in compositional range and in textural features, but in both the principal primary oxide minerals present are ilmenite and spinels.

Oxide Minerals Within Pegmatite Bodies

General Statement

As noted by Cameron and Desborough (1964, pp. 209–210), the various pegmatites, as a group, show a wide range of textures and mineral proportions, though many outcrops consist of essentially uniform material. Olivine and clinopyroxene crystals range from less than 1 mm to as much as 6 cm (olivine) or 10 cm (clinopyroxene), but average grain size in most outcrops is 2.5 cm or less. Specimens collected range from normal hand specimens to large blocks taken from inhomogeneous portions of pegmatites. Slabs cut from the latter have been used as sources of representative polished sections ranging from 2.5 cm to 15 cm in maximum dimension.

From these samples and from field study of outcrops from which they were taken, it is evident that oxide mineral contents of the pegmatites vary markedly from place to place, from nearly 100 percent to less than 1 percent. Ratios of ilmenite to spinel likewise show a wide range. Spinel is commonly the more abundant, but in a few specimens ilmenite is the more abundant or only oxide. The spinels range from optically homogeneous crystals to complex crystals consisting of magnetite, ulvöspinel, and chromian hercynite, with or without ilmenite, various combinations and proportions.

Ilmenite

Ilmenite is present mostly as anhedral crystals 0.1 to 5 mm in maximum diameter. The crystals occur

with or without spinel in aggregates that are interstitial to and molded around silicate crystals (Fig. 2a), hence appear to have formed after the silicates. The time relation of ilmenite to spinel presents problems that have been debated by numerous authors; *e.g.*, by Ramdohr (1969), Vincent (1960), Basta (1960), and Buddington and Lindsley (1964). In certain specimens from the pegmatites studied, ilmenite is the sole oxide mineral, or occurs as crystals independent of spinel, and clearly crystallized as an independent phase. In most specimens, however, ilmenite is in contact with spinel, commonly a chromium-poor magnetite-ulvöspinel. Textural relations do not indicate whether ilmenite coprecipitated with spinel or is a product of subsolidus oxidation of ulvöspinel with migration of ilmenite to grain boundaries of spinel. In a few specimens, however, ilmenite appears to be the earlier phase, because its crystal structure controls the form of magnetite (Fig. 2b).

Rhombohedral twinning in ilmenite is common. The grains are chemically homogeneous magnesian ilmenites (Table 1). Contents of V_2O_3, Cr_2O_3, and Al_2O_3 are low. MnO, determined for a few ilmenites, is a few tenths of 1 percent.

Spinels

Spinels within the pegmatite bodies are extremely varied, but three principal groups may be recognized. The simplest consists of euhedral to subhedral, optically homogeneous crystals such as those found in a specimen (Fig. 3a) from the marginal portion of the large pegmatite on the South Tweefontein-De Grooteboom boundary (Cameron and Desborough, 1964). The rock is an anorthositic norite in an advanced stage of replacement by olivine and clinopyroxene, with minor hornblende (for evidence see Cameron and Desborough, 1964, pp. 212–213). The spinel crystals in the rock are probably pseudomorphs after accessory chromite present in the replaced rocks. The 16 homogeneous spinel crystals analyzed in this rock show a range of composition with extremes as given by analyses 1 and 2 of Table 2. No. 1 is highest in Cr_2O_3. However, disseminated chromite in anorthositic norite unaffected by pegmatite has 44 to 46 percent Cr_2O_3; hence all crystals in the replaced rock have been altered. A feature unique to this specimen is the occurrence of composite crystals of the kind shown in Figure 3b. These consist of three components (analyses 3, 4, and 5, Table 2) with or without needles of rutile. All such aggregates have selvages of hornblende separating them from clinopyroxene or plagioclase. There is a strong suggestion that breakdown of titanian chromite into aluminum-rich and aluminum-poor spinels, ± rutile, is related to formation of hornblende along intergrain boundaries. The presence of rutile suggests that increase in fO_2 was a factor.

Euhedral to subhedral crystals of titanian chromite in other pegmatite specimens are likewise considered as pseudomorphs after chromite in the replaced rocks. In one specimen containing a rather sharp contact between pegmatite and anorthositic norite (Cameron and Desborough, 1964, Fig. 4), microprobe analysis shows increase in Ti and Fe and decrease in Cr, Al, and Mg in chromite crystals in the norite with decreasing distance from the contact.

TABLE 1. Analyses of Ilmenite in Pegmatites

Sample*	(1)	(2)	(3)	(4)	(5)	(6)	(7)	(8)	(9)
TiO_2	53.02	53.13	51.98	52.79	54.30	52.74	51.69	51.70	51.82
Al_2O_3	0.00	0.00	0.08	0.06	0.02	0.09	0.00	0.00	0.07
Cr_2O_3	0.05	0.08	0.04	0.03	0.01	0.05	0.08	0.04	0.02
V_2O_3	0.00	0.00	0.00	0.00	0.00	0.00	0.00	0.00	0.00
FeO	45.97	44.97	45.60	43.82	46.22	46.44	48.05	46.01	46.22
MgO	1.26	1.17	1.54	2.56	1.62	1.08	1.39	1.85	1.09
Total	100.30	99.35	99.24	99.26	102.17	100.40	101.21	99.60	99.22

*Sample descriptions:
(1) Discrete ilmenite, South Tweefontein.
(2) Same rock, ilmenite blade in magnetite-ulvospinel-hercynite intergrowth in contact with discrete ilmenite of analysis 1.
(3) Discrete ilmenite from another part of the same pegmatite body as 1.
(4) through (7), discrete ilmenites from various parts of the large pegmatite body (Cameron and Desborough, 1964) on Annex Grootboom.
(8) Discrete ilmenite, South Tweefontein.
(9) Sample from pegmatite in southern part of Annex Grootboom. Ilmenite is sole oxide mineral present.

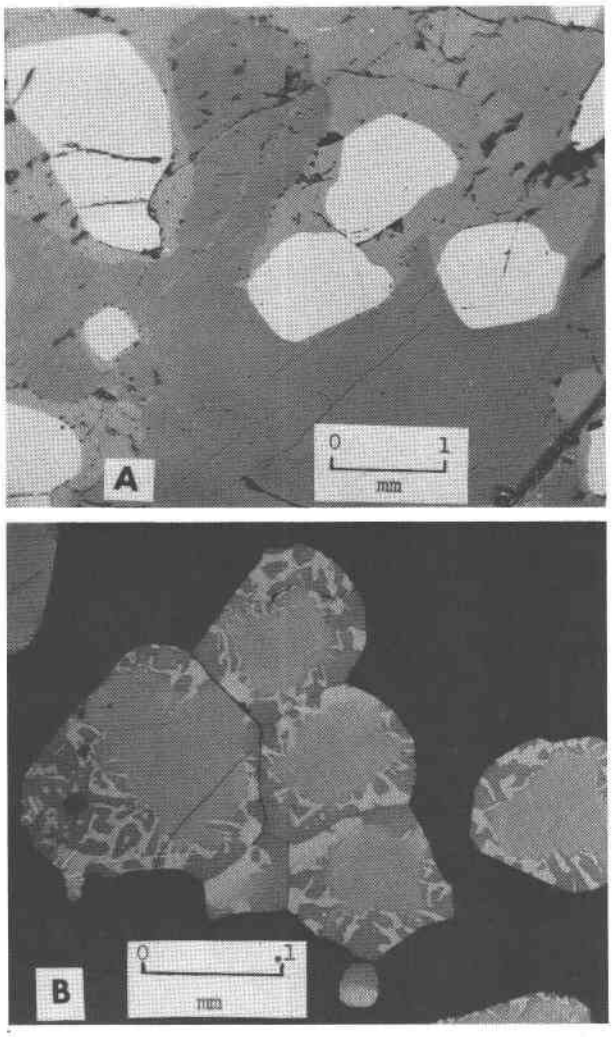

FIG. 3. (a) Euhedral to subhedral crystals of titanian chromite (white) of intermediate composition, probably pseudomorphous after Ti-poor chromite, South Tweefontein. Gray—silicates.

(b) Same section as (a), but titanian chromite crystals (medium gray) have been partly replaced by Al-rich chromite (darker gray) and Ti-rich chromite (white). Thin, straight white lines are rutile. Oil imm.

Spinels of the second group include anhedral crystals that are intergrowths of magnetite and ulvöspinel (Figs. 4a and 4b). Analyses 7, 8, 9 and 10 of Table 2 represent this type of spinel. Moderate to high contents of TiO_2, high contents of Fe oxides, and low contents of Al_2O_3, Cr_2O_3, and MgO are characteristic. Some such crystals show patchy development of fine-scale latticeworks of ilmenite, presumably due to oxidation (Vincent and others, 1957). The latticeworks have generally developed from grain margins or fractures in the crystals.

The third and commonest group of spinels consists of complex crystals (Figs. 5a, 5b, 6a). In these, the basic spinel components are magnetite and ulvöspinel in fine-scale intergrowth. Cores of the crystals contain discs of hercynite along (100), whereas rims are free of hercynite but are commonly fringed by vermicular intergrowths of ilmenite and hercynite. Where the fringes are developed along contacts of spinel with ilmenite, the latter is optically continuous with ilmenite in the fringes. Many complex spinel crystals contain ilmenite blades along (111) of magnetite-ulvöspinel (Fig. 5a). Adjacent spinel is then free of hercynite, but hercynite is finely intergrown with the ilmenite blades. There are numerous variations of the general pattern just described. In some crystals, finer-scale ilmenite appears along (111) of the main spinel. In one specimen (Fig. 6a), three sets of ilmenite blades, distinctly different in size, but all along (111) of magnetite, are present; the only spinel remaining is magnetite.

Bulk compositions of such aggregates are not readily determined with the electron microprobe, and analyses are of uncertain accuracy. Oxide summations commonly are 102 to 104 percent. However, a satisfactory summation was obtained for a magnetite-ilmenite-hercynite aggregate in one specimen (Table 2, no. 11), by analyzing 25 spots, 10 μm apart, along a line across the aggregate, using a beam about 10 μm in diameter. Counts for the individual spots were averaged. The hercynite-free rim of the same crystal was also analyzed (Table 2, no. 12). Higher Al_2O_3, lower TiO_2, higher FeO, and lower Fe_2O_3 in the core are believed to reflect the presence of hercynite discs. The discs are too small for quantitative analysis, but traverses across them indicate that they are high in Al_2O_3. In the fringes, hercynite is locally coarse enough to permit fairly accurate analysis (Table 2, no. 13). Magnesian chromian hercynite is indicated. Analyses of other aggregates, though giving high summations, show similar proportions of oxides.

The origin of aggregates of this type is partly in dispute. Hercynite intergrown with magnetite-ulvöspinel is common in terrestrial rocks and is generally ascribed to exsolution with falling temperature (*e.g.*, Ramdohr, 1969, p. 905). Inferences from microscope studies are supported by experimental evidence (Turnock and Eugster, 1962). In the rocks here described, exsolution in the interiors of the grains has yielded the discs of hercynite along (100) of the magnetite-ulvöspinel, whereas hercynite exsolved from the margins has diffused to the crystal rims.

TABLE 2. Analyses of Spinels in Pegmatites

Sample*	(1)	(2)	(3)	(4)	(5)	(6)	(7)	(8)	(9)	(10)	(11)	(12)	(13)	(14)	(15)	(16)
TiO_2	7.54	3.92	7.94	3.21	14.93	21.62	12.94	15.02	20.09	15.67	7.82	7.10	0.39	10.37	0.15	5.69
Al_2O_3	12.53	16.55	13.30	20.49	5.45	3.01	3.67	3.72	3.66	3.54	3.66	1.79	51.23	6.20	55.91	.68
Cr_2O_3	27.37	32.13	27.42	31.07	20.36	2.32	2.35	0.73	2.55	4.53	2.12	2.04	7.54	5.28	2.85	.42
V_2O_3	1.61	1.45	1.50	.81	2.01	0.65	2.93	2.22	1.12	1.52	3.69	3.90	0.28	10.20	1.56	2.68
Fe_2O_3	13.81	11.15	10.07	7.93	12.14	21.45	34.56	33.98	21.90	27.74	44.14	47.04	1.61	27.35	1.03	55.37
FeO	33.25	31.61	36.86	31.69	44.05	51.30	42.75	45.07	48.65	44.39	38.26	37.51	29.71	41.75	30.95	36.72
MgO	5.08	4.49	2.81	4.02	1.51	0.43	0.66	0.71	0.93	0.92	0.57	0.29	6.39	0.54	6.33	.22
Total	101.19	101.30	99.90	99.22	100.45	100.78	99.86	101.45	98.90	98.31	100.26	99.67	97.15	101.69	98.78	101.78

*Sample descriptions
(1) Titanian aluminian chromite, South Tweefontein.
(2) Titanian aluminian chromite, same polished section as (1).
(3), (4), (5) South Tweefontein, aggregate of Figure 3b. (3)- titanian chromite;(4)- darker component of intergrowth replacing(3);(5)-lighter component of intergrowth. Same section as (1) and (2).
(6) Euhedral magnetite-ulvospinel crystals, magnetite pyroxenite, Annex Grootboom.
(7) Magnetite-ulvöspinel, South Tweefontein.
(8) Magnetite-ulvöspinel, Annex Grootboom.
(9) Magnetite-ulvöspinel, Annex Grootboom.
(10) Magnetite-ulvöspinel, South Tweefontein.
(11) Magnetite-ulvöspinel-hercynite intergrowths forming core of crystal, South Tweefontein. Average of 25 spots, 10 microns apart, a beam approximately 10 microns in diameter.
(12) Magnetite-ulvöspinel, hercynite-free, in same crystal as (11).
(13) Magnesian aluminian hercynite, from fringe of complex spinel aggregate, Annex Grootboom.
(14) Vanadium-rich spinel, Annex Grootboom.
(15) Spinel forming euhedral crystals associated with vanadium-rich spinel of (14).
(16) Interstitial magnetite, same specimen as (14) and (15).

The origin of the large ilmenite blades parallel to (111) of magnetite-ulvöspinel is not so clear. Experimental evidence (Muan and Osborn, 1956; Buddington and Lindsley, 1964; Taylor, 1964) indicates that in the system $FeO - Fe_2O_3 - TiO_2$ the solubility of the rhombohedral phase in the cubic phase is very low, and the addition of MgO to the system (Speidel, 1970) tends to lower the solubility further. Hercynite-bearing titanomagnetites analyzed in the present study contain 8 to 12 percent $Al_2O_3 + Cr_2O_3 + V_2O_3$. The effects of these minor components on the solubility of the rhombohedral phase have not yet been established. Ramdohr (1969, pp. 901–2), however, has argued that ilmenite in some cases has formed by exsolution. Basta (1960, p. 1044) concluded that the large ilmenite blades are due to exsolution, the remainder due to decomposition or oxidation of Fe_2TiO_4.

Textural evidence is not conclusive. If the formation of the large ilmenite blades is due to oxidation, this must have occurred at the time hercynite was exsolved, because the blades contain intergrown hercynite which is not crystallographically controlled by (100) of the main spinel matrix. The vermicular ilmenite-hercynite fringes on magnetite-ulvöspinel must have formed at the same time. Later oxidation is required to account for the sets of smaller blades of ilmenite found in some such aggregates. It may or may not be significant to this problem that independent ilmenite, ilmenite in ilmenite-hercynite fringes, and ilmenite in the large discs in associated titanomagnetite all have the same composition (within the limits of analytical error). This suggests that all three textural types of ilmenite either formed under the same or closely similar conditions or were equilibrated at the time hercynite formed. In any event, formation of large ilmenite blades and fringes did not involve complete oxidation of Fe_2TiO_4. Crystals containing ilmenite only as large blades are magnetite-ulvöspinel intergrowths. These intergrowths extend unmodified through the hercynite-free bands and rims to their contacts with ilmenite; *i.e.*, the components of hercynite and ilmenite diffused to the discs and fringes, but enough Fe_2TiO_4 remained in solution in magnetite to give rise to ulvöspinel with further cooling. Ilmenite has certainly formed by oxidation of ulvöspinel in some specimens, but the common products are irregularly developed latticeworks of ilmenite and magnetite that have no relation to the large ilmenite-hercynite discs and fringe intergrowths and are totally dissimilar to the evenly developed fine-scale ilmenite of Figure 6a. Similar latticeworks have been described by Vincent and others (1957).

In several specimens, spinels occur both as euhedral or subhedral crystals and as anhedral inter-

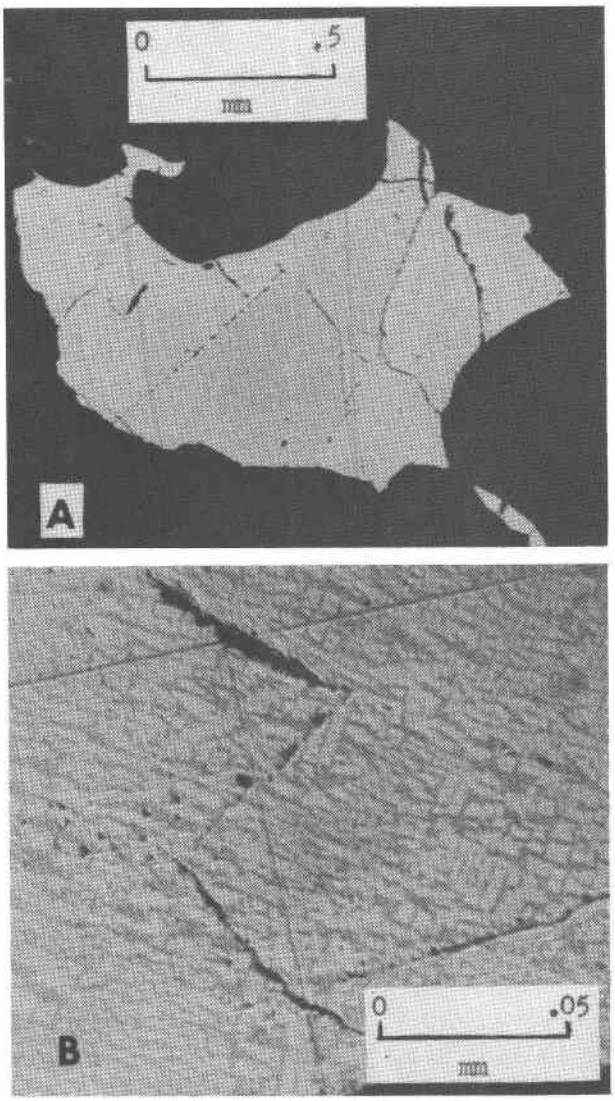

FIG. 4. (a) Magnetite-ulvöspinel anhedral and interstitial to silicates (black), Annex Grootboom.

(b) Part of same crystal, enlarged. Ulvöspinel is the darker component. Oil imm.

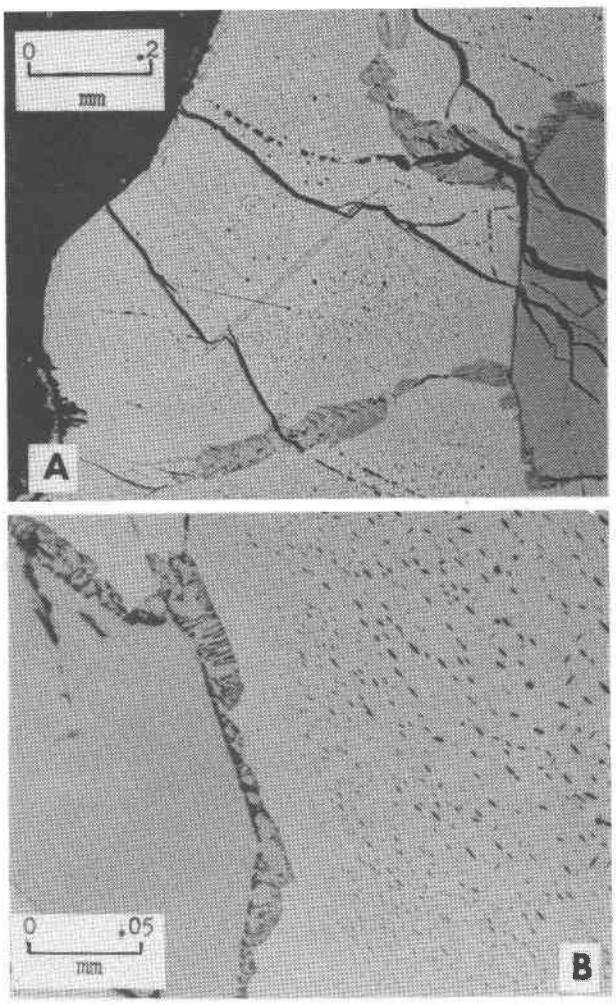

FIG. 5. (a) Complex spinel crystal (white, central area) speckled with hercynite and containing two ilmenite blades along (111). Crystal is separated from other spinel crystals above and at lower left by ilmenite (gray) finely intergrown with hercynite. Ilmenite to left is partly fringed by similar intergrowths. Black—silicates. South Tweefontein. Oil imm.

(b) Ilmenite (gray, left) fringed by optically continuous ilmenite intergrown with vermicular hercynite (darker gray to black). Remainder is magnetite-ulvöspinel containing exsolved hercynite (black) except adjacent to contact with ilmenite-hercynite. Same section as (a), oil imm.

stitial crystals or aggregates, in both cases with or without ilmenite. Two or more generations of spinels are thus suggested. A specimen of hortonolite-rich pegmatite from South Tweefontein is a clear-cut case. This rock contains three kinds of spinels (Figs. 6b, 7). The first consists of vanadium-rich euhedral to subhedral crystals, of which one (Fig. 6b; Table 2, no. 14) has the highest V_2O_3 content of any spinel we have thus far found. The second (Fig. 6b and Table 2, no. 15) is a vanadian chromian hercynite forming euhedral crystals partly enclosed in the first. A similar spinel occurs as rims on the first spinel. We suggest that the first and second spinels formed in equilibrium, but that subsequent exsolution of hercynite from the first spinel produced the rims. The third type of spinel (Fig. 7) forms grains and aggregates interstitial to silicates and is judged to have formed at a late stage of pegmatite development. Analysis 16 (Table 2) shows that it is a titanomagnetite poor in V and Al. Some crystals of the vanadium-rich spinel are marginally replaced by the titanomagnetite.

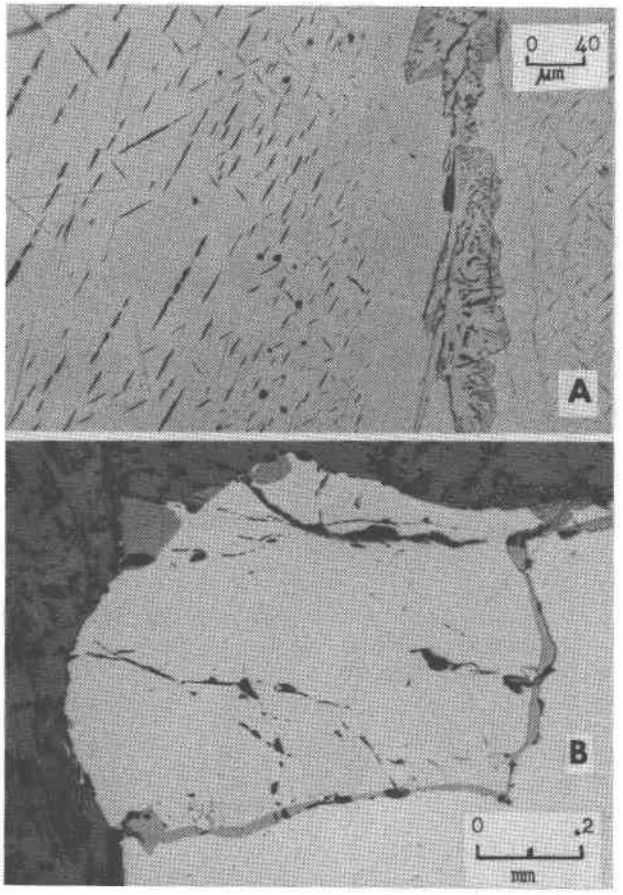

FIG. 6. (a) Complex spinel consisting of a matrix of fine-scale ilmenite and magnetite (lighter gray, not resolved at this magnification) containing exsolved hercynite (black) and a second set of ilmenite blades, slightly darker gray. Toward right, extending from top to bottom, is an intergrowth of ilmenite and vermicular hercynite (black). Annex Grootboom. Oil imm.

(b) Vanadium-rich spinel (central area) with three euhedra and a rim of hercynite (medium gray) against ilmenite (lightest gray). Darkest gray—silicates. Annex Grooboom.

Oxide Mineral Assemblages from Pegmatite-Chromitite Contact Zones

General Description

On Annex Grootboom and Spitzkop, and on the Tweefontein-De Grooteboom boundary, mafic pegmatites are in contact with one or more of the numerous layers of chromitite that characterize the Critical Zone of the eastern Bushveld Complex south of the Steelpoort River (Cameron and Desborough, 1964, 1969). From Frankel's description (Frankel, 1942) his material must have come from a pegmatite-chromitite contact zone on Tweefontein. At such a contact the outermost part of the pegmatite consists of coarse magnetic spinel with or without ilmenite. Two modes of occurrence have been found. In the simpler, magnetic spinel forms a layer along either the upper or the lower surface of a chromitite. Such layers range from 0.5 to 20 cm in thickness. Some magnetic spinel layers are even and regular, like the one along the contact between pegmatite and the M chromitite on Annex Grootboom. Other layers show irregular projections into the chromitites. The second mode of occurrence is illustrated on the hill straddling the South Tweefontein-De Grooteboom boundary. Here a chromitite seam in places has been brecciated and patchily replaced by magnetic spinel (Fig. 8), and in other places has been sheeted and replaced parallel to its contacts, so that there are now alternating layers of coarse chromian titanomagnetite and granular chromite that is enriched in iron and titanium (Fig. 9). Parts of the seam show combinations of the two mechanisms. The process is clearly a fracture-controlled but locally very irregular replacement of chromitite, and it is simply one aspect of the general process by which the mafic pegmatite bodies have developed.

A striking example of the second mode of occurrence is exposed in a gulch in the northeast part of Annex Grootboom south of the highway. There the *X* chromitite seam (Cameron and Desborough, 1964), about 2 m thick, has been replaced by zoned pegmatite along a series of fractures (Fig. 10). An outer zone consists of coarse magnetic spinel; the core, where developed, consists of coarse diallage.

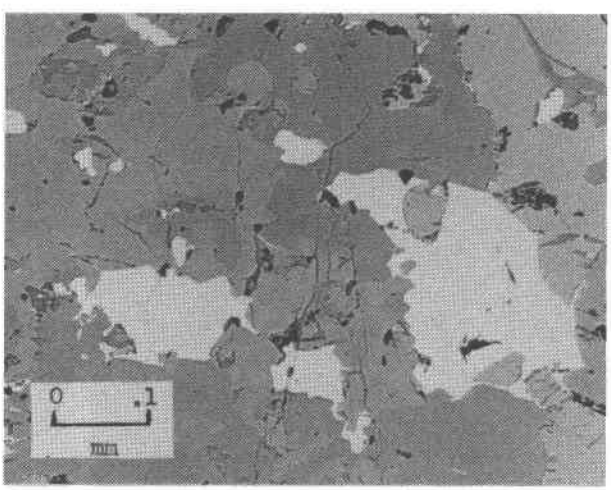

FIG. 7. Same section as 6(b). Late-formed titanomagnetite (white), interstitial to silicates (grays).

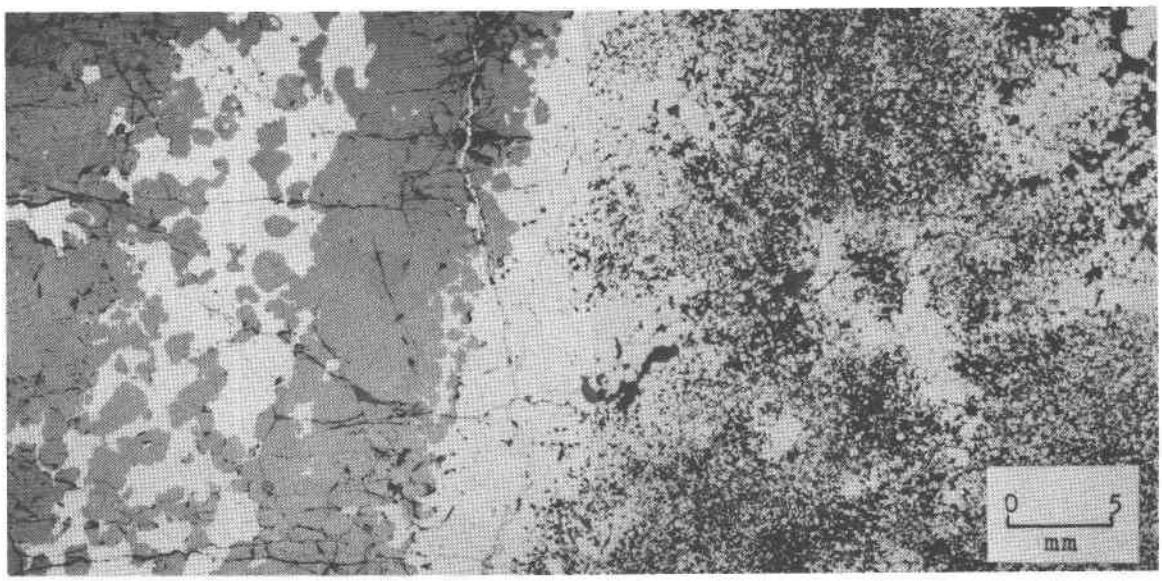

FIG. 8. Contact of pegmatite and *X* chromitite, South Tweefontein, in a polished slab. Pegmatite, at left, consists of silicates (gray) interrupted by a band of ilmenite and magnetite (white). Central band in photograph consists of magnetic spinel, which forms irregular projections into the chromitite at the right, and irregular patches in the chromitite. The latter consists of minute chromite crystals with interstitial silicates (gray). A few larger gray patches are plucked areas. Reflected light.

Boundaries of pegmatite are less definite (Fig. 11) than indicated in Figure 10, and patches of magnetic spinel appear in chromitite as much as 8 cm from the contacts.

Compositional Variations of Spinels in Contact Zones

Regardless of the mode of occurrence, polished sections and microprobe analysis show progressive

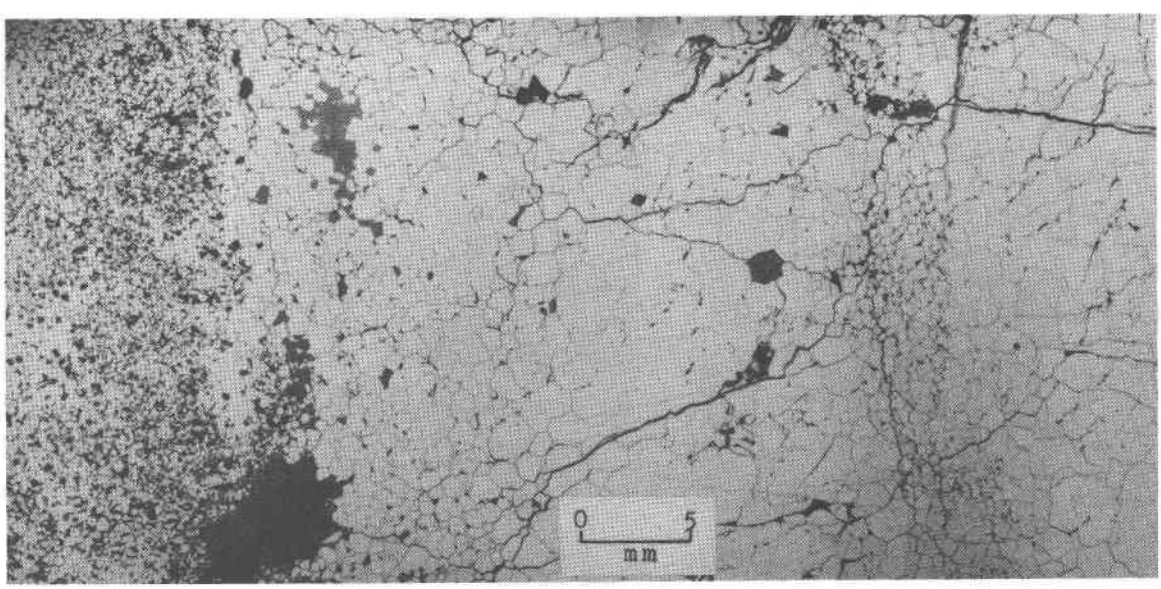

FIG. 9. Part of pegmatite-*X* chromitite contact zone, South Tweefontein. At left, fine-grained chromitite (chromite, white; interstitial silicates, gray) passing into magnetic spinel that forms alternating coarser and finer-grained layers. Probe analyses show that content of Ti and Fe varies directly as the grain size. Large gray areas are plucked. Polished slab, reflected light.

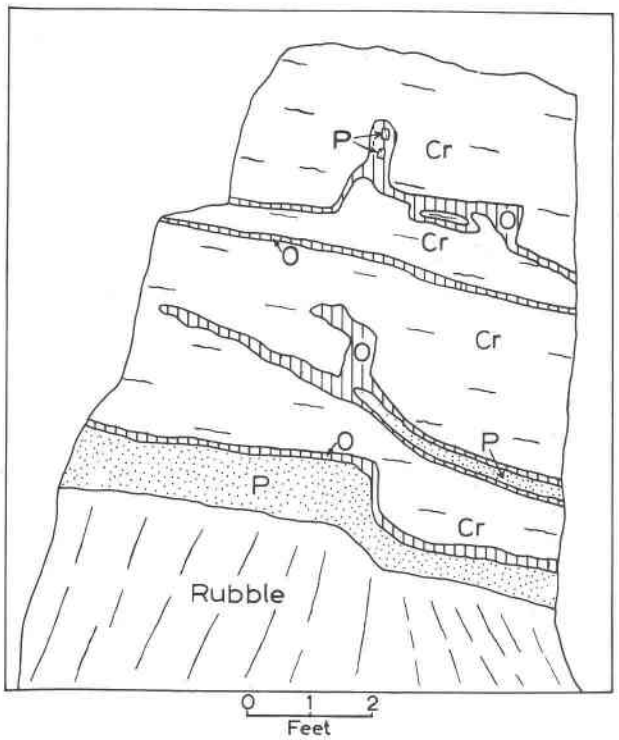

FIG. 10. Zoned pegmatite formed by replacement of *X* chromitite seam along fractures, in gulch on Annex Grootboom. C—chromitite; O—magnetic spinel zone of pegmatite; P—pyroxene zone of pegmatite.

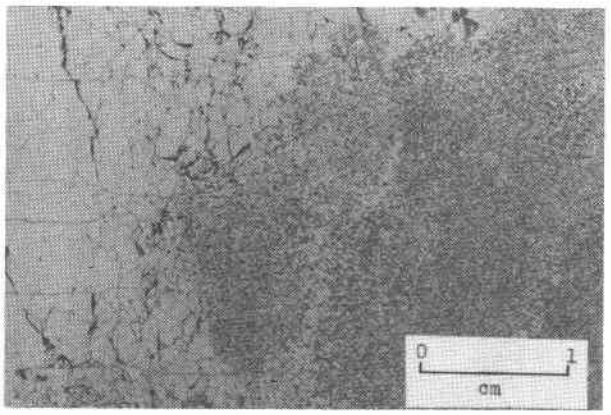

FIG. 11. Polished slab from outcrop of Figure 10. Irregular contact between magnetic spinel zone (left) and fine-grained chromite (right, speckled) consisting of chromite with interstitial silicates.

and continuous change in texture and composition along traverses extending from magnetic spinel to chromite. The typical chromitite consists of fine-grained euhedral to subhedral chromite poikilitically enclosed in bronzite or plagioclase or both. Passing from chromite across the magnetic spinel layer there is a coarsening of grain size, generally a reduction in silicate content, and a change from subhedral granular to anhedral massive oxide. Compositional changes along microprobe traverse lines are indicated in Figures 12 and 13 in terms of changes in percentages of various oxides. The progression is from Ti-poor aluminian chromite to titanomagnetite low in Cr and Al. The two profiles illustrated are typical of those found in other specimens from contact zones. Partial analyses at 10 μm intervals indicate that

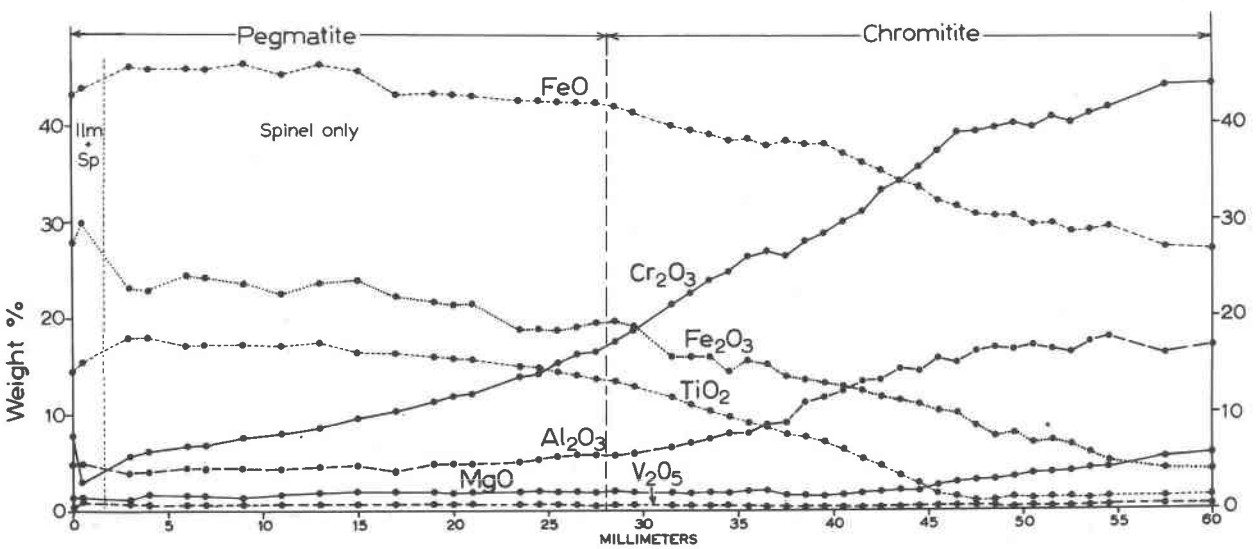

FIG. 12. Microprobe traverse from chromitite across the magnetic spinel layer of Figure 11. The long dashed vertical line is the pegmatite-chromitite contact. Each vertical line of points represents an analysis at a point along the traverse. Ilmenite coexists with spinel at points to left of the short-dashed vertical line.

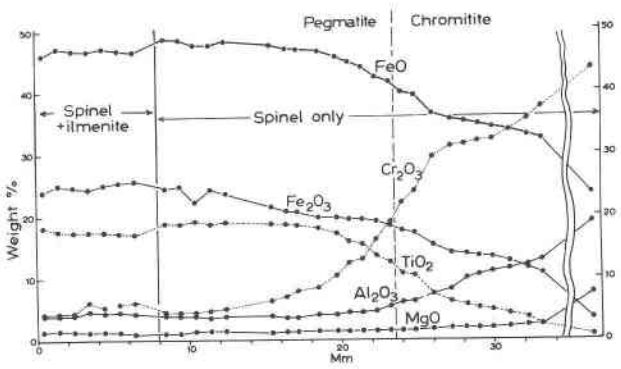

FIG. 13. Microprobe traverse across the contact of the *M* chromitite and pegmatite, Annex Grootboom. Owing to friability of the chromitite, part of the transition is missing. Analysis at the extreme right is for *M* chromitite unaffected by the pegmatite. Ilmenite coexists with spinel at points to left of solid vertical line.

there are no compositional breaks in such profiles. In Figure 13 there is a gap between unaltered chromite of the *M* seam and the first part of the profile across the adjacent contact zone. Owing to friability of the chromitite, samples obtained did not extend quite far enough into it to reach the inner edge of the transition. In the profile of Figure 12, the complete progression is shown.

In all but one of various sections across contact zones, there is a point, one to several centimeters from the apparent original contact, at which ilmenite abruptly appears (Figs. 12, 13). Simultaneously, there is an increase in the $Fe_2O_3 + Cr_2O_3$ content of the spinel phase and a decrease in FeO and TiO_2 (Figs. 12 and 13). There appears to be no fixed compositional point at which ilmenite appears but ilmenite has not been found coexisting with spinel containing more than 37 mole percent (Fe, Mg) $(Cr, Al)_2O_4$.

In Figures 14 and 15, analyses for the traverse lines of Figures 12 and 13 are plotted in terms of mole percent $Fe(Fe, V)_2O_4$, Fe_2TiO_4, and (Fe, Mg) $(Cr, Al)_2O_4$. It is clear that the compositional series can be regarded as mainly due to progressive substitution of the first two molecules for the third. With the appearance of ilmenite, however, this simple relationship breaks down. Analyzed spinels coexisting with ilmenites in contact zones plot on the Fe_2O_3 side of the main compositional trend. There are, moreover, other changes as indicated in Table 3, which gives an analysis of normal *M* chromitite and analyses and cation ratios for successive points along the traverse line of Figure 13. From chromitite to titanomagnetite, the ratio Fe^{3+}/Fe^{2+} apparently increases, Al/Cr first declines and then increases, and the Ti/Fe ratio increases.

Traverses or partial traverses across a number of pegmatite-chromitite contact zones have been made. In Figure 16, all analyses of spinels made during the present study are plotted, together with 9 analyses of spinels from elsewhere in the pegmatite bodies. Except at the Ti-rich end, spinels from pegmatite-chromitite contact zones fall within a narrow compositional band extending from near the (Fe, Mg) $(Cr, Al)_2O_4$ apex. Of the other spinels, eight (all associated with ilmenite) are from within the pegmatite bodies. These spinels are richer in $Fe(Fe, V)_2O_4$ than those from the pegmatite-chromitite contact zones. The ninth, plotting toward the chromite-hercynite apex, is from a contact zone between pegmatite and anorthositic norite.

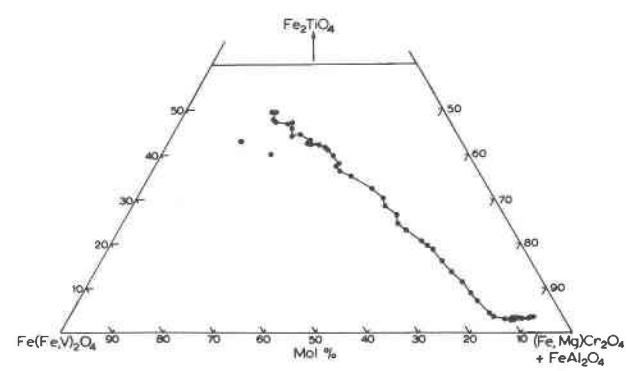

FIG. 14. Plot, in terms of selected "end members," of analyses of Figure 12. The order of connected points from lower right to upper left is their spatial order along the line of traverse.

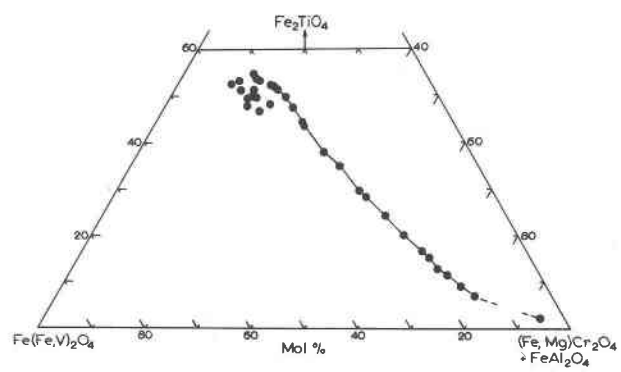

FIG. 15. Plot, in terms of selected "end members," of the analyses of Figure 13. The order of connected points from lower right to upper left is their spatial order along the line of traverse.

TABLE 3. Analyses of Spinels from Contact Zone between *M* Chromitite and Pegmatite, Annex Grootboom

Sample*	(1)	(2)	(3)	(4)	(5)	(6)	(7)	(8)	(9)	(10)	(11)	(12)**
TiO_2	0.82	2.64	4.28	5.67	7.38	10.29	12.68	13.69	15.67	17.12	18.87	18.53
Al_2O_3	19.08	12.80	11.41	10.07	7.63	6.18	5.40	5.08	4.24	4.06	3.65	3.98
Cr_2O_3	43.74	37.56	33.68	31.74	29.47	23.87	19.00	16.32	12.95	10.51	6.50	2.62
V_2O_3	0.40	0.55	0.54	0.53	0.57	0.63	0.70	0.73	0.73	0.74	0.80	1.00
Fe_2O_3	3.50	10.70	12.69	13.91	15.11	17.34	18.34	19.16	18.72	19.95	21.71	25.47
FeO	23.71	32.30	33.78	35.28	36.64	39.43	41.38	42.22	44.03	45.47	47.59	46.83
MgO	7.66	2.45	2.16	1.98	1.69	1.58	1.57	1.50	1.39	1.39	1.20	1.39
Total	98.91	99.00	98.54	99.18	98.49	99.32	99.07	98.70	97.73	99.24	100.32	99.82
						Cation Ratios						
$\frac{Fe^{3+}}{Fe^{2+}}$	.131	.298	.338	.354	.371	.396	.399	.409	.403	.395	.410	.489
$\frac{Al}{Cr}$	.650	.512	.505	.473	.386	.386	.423	.465	.488	.576	.837	2.265
$\frac{Ti}{Total\ Fe}$	.027	.057	.085	.107	.132	.168	.197	.207	.228	.243	.253	.239

*Sample descriptions: (1) Unaltered chromite. (2) to (12) Analyses of successive points in a polished section.
**At point 12, ilmenite is present.

The compositional changes shown by microprobe analysis are accompanied by systematic changes in color, reflectivity, microhardness, and unit cell size in the spinel (Cameron and Desborough, 1964). From the chromite-rich end there is a passage from gray chromite, homogeneous with respect to visible light and X-rays, to grayish pink spinel inhomogeneous to X-rays. The spinels are generally distinctly though weakly anisotropic in oil immersion. The final stage, in many specimens, is a pinkish or tan intergrowth of chromian titanomagnetite and ulvöspinel that is optically resolvable in oil immersion at high magnifications. Some such intergrowths show partial alteration to titanomaghemite. In a single section from the contact zone in the gulch on Annex Grootboom, exsolved hercynite is present in a few crystals of spinel immediately adjacent to the silicate core of the pegmatite.

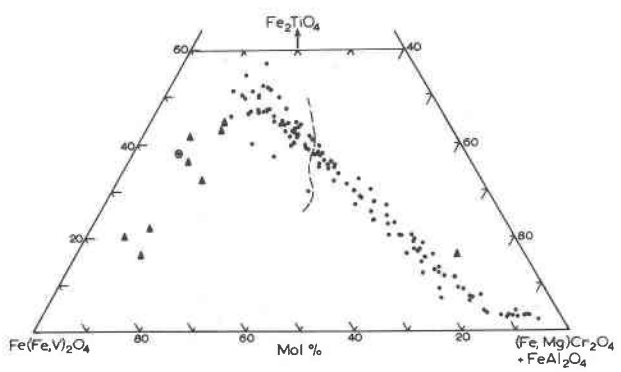

FIG. 16. Plot of various spinel analyses, in terms of selected "end members." Dots—spinels from various pegmatite-chromitite contact zones. Triangles—spinels from within pegmatite bodies. Circle with dot—titanomagnetite from the Main Magnetite Seam, Magnet Heights. Spinels to left of the broken line are almost all intergrowths; those to the right are optically homogeneous.

Occurrence and Composition of Ilmenite

In contact zones on Annex Grootboom between pegmatite and the *M* seam and *H* seam, and on Spitzkop and Tweefontein-De Grooteboom between pegmatite and the *X* seam, ilmenite has two modes of

TABLE 4. Ilmenites in Pegmatite-Chromitite Contact Zones

Sample*	(1)	(2)	(3)	(4)	(5)	(6)
TiO_2	54.74	54.55	53.51	52.75	52.92	54.87
Al_2O_3	0.00	0.05	0.00	0.00	0.00	0.04
Cr_2O_3	0.20	0.16	0.07	0.04	0.05	0.18
V_2O_3	0.00	0.00	0.00	0.00	0.00	0.00
FeO	40.63	44.18	43.37	43.28	43.91	39.84
MgO	4.79	2.04	3.08	2.73	2.76	3.61
Total	100.36	100.98	100.03	98.80	99.64	98.54

*Sample descriptions:
(1) Ilmenite from oxide layer along contact of fracture block of M chromitite and pegmatite, Annex Grootboom.
(2) Ilmenite from contact of M chromitite and pegmatite, Annex Grootboom.
(3) Ilmenite from contact zone between X chromitite and pegmatite, in gulch, Annex Grootboom.
(4) Ilmenite from contact zone between X chromitite and pegmatite, in gulch, Annex Grootboom.
(5) Ilmenite from contact zone of M seam and pegmatite, Annex Grootboom.
(6) S. Tweefontein. Ilmenite from contact zone between X chromitite and pegmatite.

TABLE 5. Analyses of "Chain" Ilmenite and Associated Spinels

Sample*	(1)	(2)	(3)	(4)	(5)	(6)	(7)	(8)	(9)
TiO_2	55.02	12.59	51.40	2.53	10.74	1.94	54.74	2.69	11.57
Al_2O_3	.01	5.63	.00	22.98	6.82	35.57	.00	22.20	7.46
Cr_2O_3	.09	14.26	.11	26.16	15.75	21.00	.20	30.21	22.04
V_2O_3	.00	1.31	.00	.50	.81	0.26	.00	.68	1.05
Fe_2O_3	---	23.08	2.33	11.86	24.04	6.56	---	8.92	15.83
FeO	40.39	40.89	41.24	30.83	38.49	26.99	40.63	29.16	38.71
MgO	3.64	1.95	3.99	4.41	2.40	8.17	4.79	5.58	3.03
Total	99.15	99.71	99.07	99.27	99.05	100.49	100.36	99.44	99.69

*Sample descriptions:
(1) Chain ilmenite, contact of pegmatite and X chromitite, south Tweefontein.
(2) Same specimen, spinel associated with ilmenite.
(3) Ilmenite from X chromitite-pegmatite contact zone, Spitzkop.
(4) Same specimen, dark spinel halo around ilmenite.
(5) Same specimen, spinel outside halo.
(6) Same specimen, chromian hercynite along boundary between spinel grains represented in analysis 5.
(7) Ilmenite from M chromitite-pegmatite contact, Annex Grootboom (Fig. 17).
(8) Same specimen, dark spinel halo around ilmenite.
(9) Same specimen, spinel outside halo.

occurrence. First, it occurs as scattered crystals or clusters of crystals that are directly in contact with Ti-Fe-rich spinel and, so far as textural relations indicate, have formed contemporaneously with that spinel. Analyses of ilmenites of this type are given in Table 4. Second, it occurs as discontinuous chains of crystals along boundaries between spinel grains, groups of the ilmenite crystals being in optical orientation with each other and, in some places, with discs or nets of ilmenite along (111) planes in spinel. Such ilmenite clearly appears to have formed by replacement of spinel, in every case an intermediate member of the titanomagnetite-chromite series. In Table 5, compositions of coexisting ilmenites and spinels having the described relation are given. Two variants are found. In one, ilmenite is directly in contact with spinel (analyses 1 and 2); in the other, the ilmenite grains have halos of a darker spinel (Fig. 17). Contacts of this spinel with ilmenite are sharp, but in some specimens contacts with normal spinel are diffuse and gradational. In Table 5, analyses of ilmenite, dark spinel, and surrounding spinel are given for a specimen from Annex Grootboom and another from Spitzkop. For the first (nos. 7–9), comparison of cation proportions in the dark spinel and in the surrounding spinel suggests a loss of divalent cations and Ti^{4+} in the correct ratio to produce ilmenite. A balanced reaction involving all cations, however, cannot be written. First, the bulk composition of a diffusion zone in the spinel immediately adjacent to the halo cannot be quantitatively determined from a two-dimensional section. Second, the pegmatite bodies and their contact zones developed by replacement in a presumably open system; hence the mineral assemblage at a given point does not necessarily represent the bulk composition of the system or even an equilibrium assemblage.

In the specimen from Spitzkop (nos. 3–5), the changes are in the same direction as those in speci-

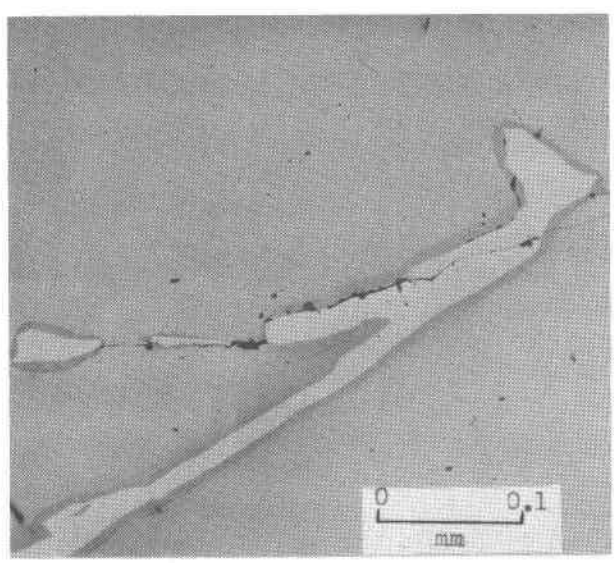

FIG. 17. Chain ilmenite (pale gray) separated from chromian titanomagnetite (medium gray) by a halo of darker spinel. Contacts of the two spinels are partly sharp, partly diffuse. Annex Grootboom, oxide layer along contact of *M* chromitite and pegmatite. Oil imm.

mens from Annex Grootboom. Besides the halos, the material from Spitzkop shows extensive development of chromian hercynite (Table 5, no. 6), without ilmenite, along fractures in spinel and along spinel grain boundaries. This hercynite is lower in Fe, Ti, and Cr, and higher in Mg and Al than the hercynite of the halos in the same specimen.

Comparison of analyses 2 and 5 indicates that the original spinels in the Tweefontein and Spitzkop specimens are essentially the same in composition, yet in the former no halo formed around the ilmenite. The reasons for the contrast between the two occurrences are not apparent.

Discussion

General Remarks

The pegmatite bodies from which the described specimens were collected are texturally and mineralogically heterogeneous. It is very unlikely that all oxide mineral relationships in these bodies have yet been discovered despite the large number of polished sections examined. Clearly, however, the characteristic oxide minerals are ilmenite and spinels ranging from chromian magnetite-ulvöspinel to aluminian chromite. There are also minor amounts of hercynite-rich spinels. The range of Cr_2O_3 content, 0.42 to 44.0 wt percent, is remarkable.

Most of the compositional range is in zones of contact between pegmatite and chromitite; interstitial spinels within pegmatites (Table 2, nos. 7–12, and 16), though showing a considerable range in ratio of Ti to Fe, are low in Cr, Al, and Mg. The less common euhedral spinels within pegmatites thus far analyzed, however, show a broader range of Cr + Al + Mg than the interstitial spinels. The euhedral spinels, however, occur along or within zones of contact between host rocks and pegmatites and represent intermediate stages in the conversion of original chromite to titanomagnetite. Analysis of euhedral spinels in additional samples will probably reveal an even broader compositional range, perhaps approaching that of the spinels in the pegmatite-chromitite contact zones. In any case, it is clear that the origin of the greater part of the known compositional range lies in processes operative in the contact zones.

Processes at work were evidently complex. The host rocks of the pegmatites are rocks of the Critical Zone of the eastern Bushveld Complex, a sequence of thick layers of norite, anorthosite, and pyroxenite separating the much thinner chromitite layers. Detailed field and laboratory investigations (Cameron and Desborough, 1964) have shown that these rocks were already completely solidified at the time the pegmatites were formed by replacement of parts of the layered sequence, especially layers of anorthosite and norite. The obvious control of replacement by grain boundaries and fractures indicates that fluids were responsible. The magmatic rocks consist of bronzite, plagioclase (*ca* An_{73}), and chromite, in various proportions. Where pegmatite bodies were formed, at some unknown time after magmatic processes terminated, the minerals cited were replaced by combinations of hortonolite, clinopyroxene, titanomagnetite, ilmenite, and plagioclase (An_{83} to An_{97}). Hornblende and biotite were formed locally in minor amounts. The initially stable assemblage was bronzite-plagioclase-chromite. The final stable assemblage was hortonolite-clinopyroxene-titanomagnetite-ilmenite, ± plagioclase ± hornblende ± biotite. Intermediate assemblages are preserved in the zones of contact between pegmatite and preexisting rocks, and it is in these zones that spinels of intermediate composition were formed.

As replacement advanced to the chromitite contacts, locally extending into the chromitites along fractures, chemical gradients were established between pegmatite and chromitite. Fe and Ti, with minor V, diffused from the pegmatites into the chromitites, progressively replacing Cr, Al, and Mg. Diffusion proceeded from the surfaces of the chromitite seams and from fractures developed in the seams. Chromite was progressively altered for distances up to at least 75 mm, and at the same time layers of spinels richer in Ti and Fe were developed in pegmatite along contacts with chromitite or in fractures in chromitite. Chromite grains nearest original contacts were somewhat enlarged during the process of enrichment in Ti and Fe. In actual specimens, the distinction between diffusion and bodily replacement is not clear, nor are the timing and mechanism of diffusion. Diffusion of ions through fluids penetrating chromitite along grain boundaries may have been involved, but diffusion in the solid was evidently an important process. The evidence is shown in Figure 18. The isopleths of the diagram are parallel to the contact zone. They are not disturbed by present grain boundaries, which are indicated by physical discontinuities and by weak anistropism of differently oriented crystal units. Either present grain structure is due to recrystallization (perhaps due to cooling

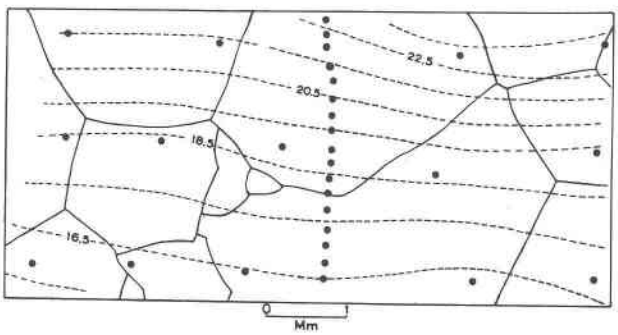

FIG. 18. Variation in Cr_2O_3 content in a small part of the spinel layer forming the contact zone between the *M* chromitite and pegmatite, Annex Grootboom. Length of diagram is parallel to the contact zone. Dashed lines are isopleths; solid lines are grain boundaries. Dots mark points for which Cr_2O_3 was determined. Supplementary scans confirm the pattern of variation of Cr_2O_3.

stress in the newly formed coarse spinel), or diffusion proceeded independently of grain boundaries. While the latter may seem unlikely, the fact is that compositional gradients are found in single crystals in the chromium-rich portion of the contact zone, which has a texture that appears to be inherited from the original chromitite.

The abrupt appearance of ilmenite in the innermost parts of contact zones can be attributed (*cf* Taylor, 1964, Fig. 2) either to increasing ratio of Ti to Fe at constant oxygen fugacity, or to increase in oxygen fugacity at constant Ti/Fe ratio, or both. Table 3 and Figure 13 show that the Ti/Fe ratio in spinel increases steadily from chromitite toward the pegmatite; until ilmenite appears at point 12. The Fe^{3+}/Fe^{2+} ratio first rises to a point about midway along the traverse, then is essentially constant until ilmenite appears. Since temperatures of formation are not known, no firm conclusions as to conditions can be drawn from the cation ratios. It is clear, however, that the Ti/Fe ratio was relatively high in the pegmatite fluids, and fO_2 was sufficiently high to cause oxidation of part of the Fe in chromite.

Subsolidus Phase Relations in the Chromite-Titanomagnetite Portion of the Spinel System

In Figure 16, spinels to the left of the broken line are almost all intergrowths, but those to the right are all optically homogeneous. Miscibility in the spinel series at low temperatures (or at least down to temperatures at which diffusion is negligible) over a broad range of composition is therefore suggested, although the range is less broad than in the ferroan counterpart series of spinels found in lunar rocks (Cameron, 1971a; Champness, *et al.*, 1971; Reid, 1971). The region of immiscibility toward the $Fe(Fe, V)_2O_4 - Fe_2TiO_4$ join is to be expected from the results of many previous investigations of Fe-Ti spinels.

Figure 16 has obvious limitations. The choice of "end members" largely conceals variations of individual cations and cation ratios (see, however, Table 3). The distinctions between homogeneous and inhomogeneous spinels is based on optical observations alone, and X-ray analysis would probably indicate a broader field of immiscibility. Breakdown of solid solutions is sensitive to various factors, and some homogeneous spinels may actually be metastable at low temperatures. Finally ,the products of breakdown are not the same in all spinels that fall within the immiscibility field. The diagram, nonetheless, has some value. It summarizes the analyses of spinels from a large number of pegmatite specimens from various localities within five different pegmatite bodies. In all five the compositional ranges of homogeneous *vs* inhomogeneous spinels, so far as these have been determined, are roughly the same. This at least suggests that metastability is not a serious factor.

A comparison of the spinel series here reported with spinel series found in lunar rocks suggests that miscibility is strongly influenced by the oxidation state of iron. In lunar rocks ferric iron is absent, and a complete solid solution series from Ti-poor aluminian chromite to nearly pure ulvöspinel is found (Cameron, 1971a; Champness, *et al.*, 1971; Reid, 1971). In the rocks here described, ferric iron is present, and immiscibility occurs over a broad region extending from the Fe_2TiO_4-$Fe(Fe,V)_2O_4$ join. On the other hand, there is no evidence of a relation between V_2O_3 content and immiscibility. Homogeneous spinels containing up to 10 percent V_2O_3 (Table 2, no. 14) occur in the pegmatites.

The role of aluminum in subsolidus immiscibility is not fully indicated by the data. As would be expected from previous studies of titanomagnetites, exsolved hercynite is present in spinels that plot near the $Fe(Fe, V)_2O_4$-Fe_2TiO_4 boundary of Figure 16. From experimental work, Muan *et al.* (1971) report extensive miscibility gaps along the Mg_2TiO_4-$MgAl_2O_4$ and Fe_2TiO_4-$FeAl_2O_4$ joins, whereas there is continuous solid solution along the analogous joins with Cr_2O_3 instead of Al_2O_3. The spinels here described were formed in ferrian systems; hence the applicability of the experimental data is doubtful. Nonetheless, except for the spinel represented by

analysis 5, Table 5, spinels with moderate to high Cr_2O_3 contents are optically homogeneous.

Relations of Pegmatite Spinels to Normal Spinels of the Bushveld Complex

The layered pile of the Bushveld Complex is famous for its remarkable accumulations of spinel minerals. These are of two kinds, occurring in different parts of the layered succession. Cumulus chromite occurs, both as an accessory mineral and in chromite-rich layers, in a stratigraphic thickness of as much as 6,000 feet of rocks that form the Critical and Transition Zones of the lower part of the Complex (Cameron and Desborough, 1969). Cumulus titanomagnetite occurs similarly in the upper 8,000 feet of the Complex (Willemse, 1969a). Some thousands of feet of layered rocks of the middle part of the Complex, however, contain no cumulus spinel (Willemse, 1969a, 1969b).

The chromites plot near the hercynite-chromite apex of a diagram such as that of Figure 16, whereas the titanomagnetites plot near the side opposite that apex. Spinels intermediate between chromite and titanomagnetite are thus absent from the normal rocks of the Bushveld. Irvine (1967) has suggested that the onset of crystallization of cumulus clinopyroxene, which can incorporate Cr_2O_3 in its lattice, can terminate the crystallization of chromite. Dickey, Yoder, and Schairer (1971) have shown that chromian diopside at 1 atm melts incongruently to spinel + liquid. In the eastern Bushveld, bronzite was the stable cumulus pyroxene during crystallization of the Transition Zone and most of the Critical Zone. In the few units in the upper part of the latter zone in which cumulus clinopyroxene is present, chromite is lacking (Cameron and Desborough, 1969; Cameron, 1971b). A short distance above the Merensky Reef, chromite disappears as clinopyroxene becomes prominent. Spinel crystallization was thus terminated and was not resumed, apart from trace amounts of postcumulus magnetite, until thousands of feet of rocks had accumulated and the concentrations of Ti and Fe in the rest magma became high enough to cause titanomagnetite to form.

The appearance of cumulus clinopyroxene thus appears to offer a reasonable explanation of the lack of cumulus spinel in the middle part of the Complex and hence of the absence of spinels of intermediate composition. In lunar rocks from Apollo 12 (Cameron, 1971a) chromite crystallization similarly ceased with the appearance of chromian clinopyroxene. There has remained, however, the possibility that the compositional gap is due to a miscibility gap, at magmatic temperatures, in the chromite-titanomagnetite series. The present findings indicate that no such gap exists, and the inference as to the role of clinopyroxene is strengthened.

There are, however, peculiar features of the occurrence of TiO_2 in Bushveld spinels. TiO_2 in normal Bushveld chromites does not exceed 2 percent. Microscope study and probe analysis show that some chromites containing TiO_2 are homogeneous, whereas others of similar bulk composition contain "exsolved" rutile, suggesting that the miscibility of TiO_2 in chromite is very limited under certain conditions. It is noteworthy, however, that there appears to be no correlation between TiO_2 content and the presence or absence of an "exsolved" titanium phase. Moreover, in some chromitite layers, "exsolved" rutile is present in certain grains but not in others. We suggest, therefore, that the presence or absence of rutile is a function of the range of oxygen fugacity to which particular chromite grains have been subjected since accumulation. With sufficient increase in fO_2 after accumulation, a TiO_2 phase could form (Taylor, 1964) by oxidation of Fe_2TiO_4 present in chromite.

Summary of Findings

1. Mafic pegmatites of the eastern Bushveld Complex contain a series of spinels ranging from Ti-poor aluminian chromite to Cr-poor titanomagnetite. The broadest range of composition is found in pegmatite-chromitite contact zones.
2. The spinels are a ferrian counterpart of the ferroan series of titanian-chromian spinels found in lunar igneous rocks.
3. Layers of oxide minerals along pegmatite-chromitite contacts resulted from reactions of fluids rich in Ti and Fe with chromite rich in Cr, Al, and Mg. Metasomatic replacement was followed by solid diffusion of cations along chemical gradients between pegmatites and chromitites.
4. The chromite-titanomagnetite series is characterized by a broad range of miscibility at relatively low temperatures.
5. The existence of spinels intermediate in composition between titanomagnetite and chromite lends support to the inference that the absence of such spinels in the normal layered sequence of the Bushveld Complex is related to the appearance and long continued crystallization of cumulus clinopyroxene.

Acknowledgments

The authors express their deep appreciation to Dr. Hatten S. Yoder, Jr., for numerous helpful comments and criticisms based on his thoughtful review of the manuscript.

References

BASTA, E. Z. (1960) Natural and synthetic titanomagnetites (the System Fe_3O_4-Fe_2TiO_4-$FeTiO_3$). *Neues Jahrb. Mineral. Abh.* **94,** 1017–1048.

BUDDINGTON, A. F., AND D. H. LINDSLEY (1964) Iron-titanium oxides and synthetic equivalents. *Jour. Petrology,* **5,** 310–357.

CAMERON, E. N. (1971a) Opaque minerals in certain lunar rocks from Apollo 12. *Proc. Second Lunar Sci. Conf.* **1,** 193–206.

—— (1971b) Problems of the eastern Bushveld Complex. *Fortschr. Mineral.* **48,** 86–108.

———, AND G. A. DESBOROUGH (1964) Origin of certain magnetite-bearing pegmatites in the eastern part of the Bushveld Complex, South Africa. *Econ. Geol.* **59,** 197–225.

———, AND ——— (1969) Occurrence and characteristics of chromite deposits—eastern Bushveld Complex. *Econ. Geol. Mon.* **4,** 23–40.

CHAMPNESS, P. S., A. C. DUNHAM, F. G. F. GIBB, H. N. GILES, W. S. MACKENZIE, E. F. STUMPFL, AND J. ZUSSMANN (1971) Mineralogy and petrology of some Apollo 12 lunar samples. *Proc. Second Lunar Sci. Conf.* **1,** 359–376.

DICKEY, J. S., JR., H. S. YODER, JR., AND J. F. SCHAIRER (1971) Chromium in silicate-oxide systems. *Carnegie Inst. Washington Year Book,* **70,** 118–122.

EVANS, B. W., AND J. G. MOORE (1968) Mineralogy as a function of depth in the prehistoric Makaopuhi tholeiitic lava lake, Hawaii. *Contrib. Mineral. Petrology,* **17,** 85–115.

FRANKEL, J. J. (1942) Chrome-bearing magnetic rocks from the eastern Bushveld. *S. African J. Sci.* **38,** 152–157.

IRVINE, T. N. (1967) Chromian spinel as a petrogenetic indicator. Part 2. Petrologic applications. *Can. J. Earth Sci.* **4,** 71–103.

MUAN, A., AND E. F. OSBORN (1956) Phase equilibria at liquidus temperatures in the system MgO-FeO-Fe_2O_3-SiO_2. *J. Amer. Ceram. Soc.* **39,** 121–140.

———, J. HAUCK, E. F. OSBORN, AND J. F. SCHAIRER (1971) Equilibrium relations among phases occurring in lunar rocks. *Proc. Second Lunar Sci. Conf.* **1,** 497–505.

RAMDOHR, P. (1969) *The Ore Minerals and Their Intergrowths.* Pergamon Press, London. 1174 pages.

REID, JOHN B., JR. (1971) Apollo 12 spinels as petrogenetic indicators. *Earth Planet. Sci. Lett.* **10,** 351–356.

SPEIDEL, D. H. (1967) Phase equilibria in the system MgO-FeO-Fe_2O_3: The 1300°C isothermal section and extrapolation to other temperatures. *Amer. Ceram. Soc. J.* **50,** 243–248.

——— (1970) Effect of magnesium on the iron-titanium oxides. *Amer. J. Sci.* **268,** 341–353.

———, AND E. F. OSBORN (1967) Element distribution among coexisting phases in the system MgO-FeO-Fe_2O_3-SiO_2 as a function of temperature and oxygen fugacity. *Amer. Mineral.* **52,** 1139–52.

TAYLOR, R. W. (1964) Phase equilibria in the system FeO-Fe_2O_3-TiO_2 at 1300°C. *Amer. Mineral.* **49,** 1016–1030.

TURNOCK, A. C., AND H. P. EUGSTER (1962) Fe-Al oxides: Phase relations below 1000°C. *J. Petrology,* **8,** 533–565.

VINCENT, E. A. (1960) Ulvöspinel in the Skaergaard intrusion, Greenland. *Neues Jahrb Mineral. Abh.* **94,** 993–1016.

———, J. B. WRIGHT, R. CHEVALIER, AND S. MATHIEU (1957) Heating experiments on some natural titaniferous magnetites. *Mineral. Mag.* **31,** 624–655.

WILLEMSE, J. (1969a) The geology of the Bushveld Igneous Complex, the largest repository of magmatic ore deposits in the world. *Econ. Geol. Mon.* **4,** 1-22.

——— (1969b) The vanadiferous magnetic iron ore of the Bushveld Igneous Complex. *Econ. Geol. Mon.* **4,** 187-208.

Manuscript received, August 11, 1972; accepted for publication, November 21, 1972.